On the dynamic response of laminated glass exposed to impact before blast loading

K. Osnes[a,b,*], S. Dey[c], O. S. Hopperstad[a,b], T. Børvik[a,b]

[a]*Structural Impact Laboratory (SIMLab), Department of Structural Engineering, NTNU, Norwegian University of Science and Technology, NO-7491 Trondheim, Norway*
[b]*Centre for Advanced Structural Analysis (CASA), NTNU, Norwegian University of Science and Technology, NO-7491 Trondheim, Norway*
[c]*Norwegian Defence Estates Agency, Research and Development Department, NO-0105 Oslo, Norway*

Abstract

In this study, the effect of fragment or bullet impact before blast loading on laminated glass is studied experimentally. First, laminated windows consisting of two 3.8 mm thick annealed float glass plates and a 1.52 mm thick PVB interlayer were blast loaded in a shock tube with various pressures as a reference. In these tests, the blast loading was successively increased until fracture occurred not only in the glass plates but also in the PVB interlayer. Second, a diamond drill was used to make a 5 mm diameter centrally placed hole in some windows before they were blast loaded with the same pressures as those used for the undamaged windows. Third, windows were impacted by 7.62 mm AP bullets, both with and without the brass jacket, before they were blast loaded. Such bullets may have similar mass and velocity to typical primary fragments from an explosive detonation. The results are finally compared with each other and discussed with respect to the blast protection offered. It is found that the capacity is significantly reduced if the laminated glass is perforated by a fragment or a bullet before it is blast loaded and that such impacts should be considered in the design of blast-resistant windows.

Keywords: Laminated glass, impact tests, blast tests, glass fracture, PVB failure

*Corresponding author
Email addresses: karoline.osnes@ntnu.no (K. Osnes), Sumita.Dey@forsvarsbygg.no (S. Dey), odd.hopperstad@ntnu.no (O. S. Hopperstad), tore.borvik@ntnu.no (T. Børvik)

1. Introduction

Ordinary windows used in buildings typically consist of two layers of annealed float glass separated by a layer of argon gas. The glass material is highly brittle and offers limited resistance to extreme loading conditions such as high-velocity impacts or blast waves generated by explosions [1]. Due to the lack of plastic deformation, the energy dissipated during crack propagation in glass is small, and the fracture propagates fast with little chance of crack arrest [2]. Thus, ordinary window glass will break into numerous sharp fragments that may travel at high velocities and potentially cause severe damage to the surroundings when they are exposed to extreme loadings. One way of reducing this risk is to apply laminated glass, which is a type of safety glass extensively used by e.g. the automotive industry as windshields or in protective structures for blast mitigation.

A laminated glass is simply made by sandwiching layers of polyvinyl butyral (PVB) or other structural interlayer materials in between two or more plates of annealed or strengthened float glass. The components are bonded permanently using both mechanical and chemical bonds. The main intention of the interlayer is to keep the sharp glass pieces bonded if the window breaks. Furthermore, the interlayer's low stiffness and ability to deform ensure that the glass breaks into small pieces instead of large and sharp fragments. Another very important feature of the interlayer is that it provides additional resistance even after the glass plates have fractured [3–5]. This property is particularly important in blast protection, as it prevents the blast pressure from entering the building. If the blast pressure is allowed to freely enter any part of the building, it may be a severe threat to both the occupants and the structural integrity. This hazard was demonstrated during the terrorist attack against the Executive Government Quarter on the 22$^{\text{th}}$ of July, 2011, in Oslo, Norway (see, e.g., [6]), where only a few of the windows in the façade were blast protected.

Whenever a chemical explosive detonates, a shock wave is generated and followed by a series of pressure waves, thus forming a blast wave. The detonation velocity is very high (typically several thousands of meters per second), and the blast wave propagates outwards from the source into the surrounding air. As the blast wave expands, it decays in intensity, increases in duration and decreases in velocity. The decrease in pressure occurs rapidly (approximately with the cube of the distance) due to geometrical effects and energy dissipation caused by heating of the air [7]. The

blast wave is most often accompanied by primary and/or secondary fragments. Primary fragments are defined as parts initially contained in the explosive device (e.g., ball bearings) or parts from the fractured casing of the explosive (e.g., a shell or a vehicle), while secondary fragments are external objects picked up by the blast wave along its path. The primary fragments propagate with a high and rather constant velocity (up to several kilometres per second), having masses ranging from less than a gram to tens of grams [8–11]. The technical manual TM5-855 [8] reports expected average masses and velocities (from a warhead casing of 420 kg) ranging from 1.7 g to 83.1 g and 745 m/s to 1509 m/s, respectively. Arnold et al. [9] studied casings of different thicknesses and materials, and reported fragment masses from around 0.001 to 100 g. Field tests by Grisaro et al. [10], involving cased charges of approximately 11 kg, resulted in fragment masses up to 5 g and velocities ranging from approximately 1100 to 2053 m/s. The study by Guo et al. [11] on different explosive-filled casings recorded fragment velocities of approximately 950 to 1600 m/s. Typical examples of secondary fragments include building debris or loose items on the ground, and they have in general a much lower velocity and a higher mass than primary fragments.

If the detonation is close-in, the shock wave may hit the structure before the fragments, while if the detonation is far-field, it is likely that the fragments will arrive before the shock wave. Under certain conditions, the shock wave and the fragments will arrive simultaneously, so the structure experiences the combined effect of impact and blast loading [12, 13]. What the outcome will be is a function of a number of factors, such as type of explosive/casing, standoff distance and weight of explosive/casing. This issue is still an open research topic [14–16]. An example of the detonation of a vehicle-borne improvised explosive device (VBIED), revealing the shock wave, the fragments and the fireball, is shown in Figure 1. From this picture, it can clearly be seen that numerous fragments are propagating in front of the shock wave. Therefore, what happens with the blast protection if a fragment hits a laminated glass before the shock wave? Since high-velocity impact is a highly localized process, it is very likely that the fragment will break the glass plates and perforate the interlayer. This effect may allow the blast wave to rupture the laminate and enter the building when it arrives shortly after the impact. To the best of the authors' knowledge, the combined effect of fragment and blast loading on laminated glass has not been previously reported in the open literature. Thus, in this study, the effect of impact before blast loading on

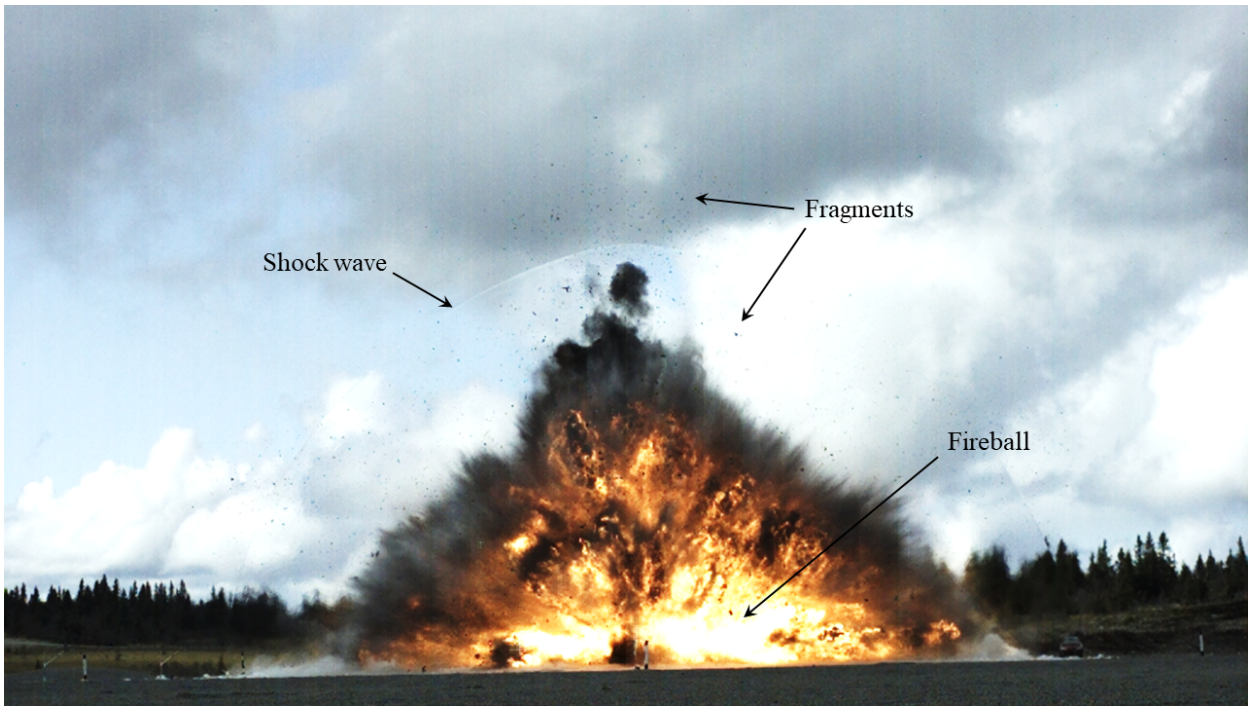

Figure 1: Combined blast and fragment loading after detonation of a vehicle-borne improvised explosive device (VBIED). Courtesy of the Norwegian Defence Estate Agency (Forsvarsbygg).

laminated glass was studied experimentally. First, laminated windows consisting of two 3.8 mm thick annealed float glass plates and a 1.52 mm thick PVB interlayer were blast loaded in a shock tube at various pressures as a reference. In these tests, the blast loading was successively increased until fracture occurred not only in the glass plates but also in the interlayer. Second, a diamond drill was used to make a 5 mm diameter centrally placed hole in the windows before they were blast loaded with the same pressures as those used for the initially undamaged windows. Third, windows were impacted by 7.62 mm armour-piercing (AP) bullets, both with and without the brass jacket, before they were blast loaded. Such bullets may have similar mass and velocity to typical primary fragments (see, e.g., [9–11]). The results were finally compared with each other and discussed with respect to the blast protection offered. It is found that the degree of protection is significantly reduced if the laminated glass is perforated by fragments before it is blast loaded, and that the blast-resistant window design could give non-conservative results if the effects of fragment impact are not properly accounted for.

2. Materials

2.1. Annealed float glass

The glass plates used in this study are made of clear annealed soda-lime-silica float glass. Such glass plates are manufactured as large sheets (typically 3.21 m $\times$ 6 m [17]) by pouring molten material on a liquid tin bath where it solidifies in a controlled manner. The liquid tin ensures the uniform thickness of the sheets, and the dimensions are adjusted by stretching or compressing the molten material. The tin temperature is then lowered in a controlled manner until the glass sheet has hardened. This annealing process is important to relieve internal residual stresses introduced during manufacturing. Annealed float glass is a brittle material and has linear elastic behaviour to the point of failure. Fracture in glass typically initiates at microscopic flaws located on the surface, causing the fracture strength to be highly stochastic [18]. Since the opening of a flaw is the predecessor to crack propagation, glass plates primarily fail in tension [19]. Commonly used material parameters for float glass are found in the European Standard NS-EN 572-1 [20]. It reports a density of 2500 kg/m^3, an elastic modulus of 70000 MPa, and a Poisson's ratio of 0.2. The fracture toughness of glass is reported in Anstis et al. [21], based on quasi-static tests by Wiederhorn [2]. The value is stated as 0.75 MPa$\sqrt{\text{m}}$ and correlates with the critical stress intensity factor for mode I loading, i.e., the opening of a flaw. It should, however, be mentioned that the fracture strength of glass is strain rate sensitive [22, 23], which could affect the fracture toughness.

2.2. PVB

The laminated glass used in this study includes an interlayer of polyvinyl butyral (PVB), which is the most commonly used interlayer in laminated glass [5]; however, other materials can also be used (such as ionoplast, polycarbonate and similar materials). PVB displays highly non-linear and time-dependent behaviour and may undergo large strains before failure. The material has a viscoelastic behaviour, and exhibits a different response under low and high strain rates [24, 25]. It should be noted that there is close to no permanent deformation of the PVB material a sufficient amount of time after loading [25]. Furthermore, PVB is a nearly incompressible material [3] and is also highly temperature dependent [26].

2.3. Laminated glass

Laminated glass is a combination of two or more glass plates bonded together with a polymer interlayer (usually PVB). Normally several layers of 0.38 mm thick PVB films are used. If the glass breaks, the glass fragments are contained on the surface of the polymer, offering an increased level of protection against impact and blast loading. The post-fracture behaviour of laminated glass is a complicated process that depends on many different factors. Delamination will occur between the glass and the polymer, which in turn allows stretching of the interlayer [5]. If the interlayer is flexible, as in the case of PVB, it can deform significantly and absorb energy. If the applied load is sufficiently large, detachment of glass fragments can occur. This effect is dependent on the adhesion level, which in turn depends on the production process [27]. The production of laminated glass involves at least five main steps: (1) The glass is cut into required shapes, designs and sizes following given specifications. (2) Using feeding devices and a roller table, the glass is conveyed to washing machines. In this stage, wider gaps between glass panes are automatically minimized. (3) The glass panes are thoroughly cleaned and dried using automated machines. (4) The clean and dry glass panes are transferred to a clean room with conditioned temperature and humidity, where the PVB film rolls are stored. Together with the PVB films, the glass panes are accurately aligned according to their geometry. The laminated glass is then placed on a nip roller where it is heated and compressed simultaneously to remove air in between the layers. (5) The nipped specimen is transferred to the autoclave cart. In this final stage, controlled cycles of heat and pressure are applied to adhere the layers together and make the laminated glass clear.

3. Experimental setups

3.1. Ballistic impact tests

In an attempt to mimic an impact of a primary fragment from an explosion, two different approaches were exploited. First, a glazier used a 5 mm diameter diamond drill to make a hole in the centre of the laminated glass. This process could be performed without damaging the glass plates outside the central region, except maybe for some micro-cracks not visible to the naked eye. Two laminated windows were tested in this configuration. Second, a smooth-bored Mauser rifle

was used to fire 7.62 mm armour-piercing (AP) bullets at the centre of the laminated glass plates. A total of four laminated windows were impacted by bullets. The applied AP bullet consists of a brass jacket, a lead tip, an end cap and a hardened steel core [28, 29]. The mass of the hardened steel core is 5 $\pm$ 0.25 g, while the mass of the whole bullet is 10.5 $\pm$ 0.25 g. The dimensions of the bullet are given in Figure 2a. In two of the tests, only the hard core of the AP bullet was used to impact the laminated glass. In this case, the 6.1 mm diameter hard steel core was encased in a 0.3 g plastic sabot before inserted into the cartridge [30, 31]. The ammunition was adjusted by removing some of the powder before firing the core-only (CO) bullet, with the intention of having approximately the same initial velocity for the CO and AP bullets. It is assumed that the hardened steel core, having a Rockwell C hardness of 63, will not considerably deform as a result of the impact.

During testing, the laminated glass plate was clamped at the top and bottom between steel platens with 4 mm thick Neoprene rubber strips in between, as shown in Figure 2b. Each test was recorded with a Phantom v2511 high-speed camera with a recording rate of 100,000 fps. Both the initial and the residual velocity of the bullet were measured using a point-tracking procedure in the digital image correlation (DIC) software eCorr [32]. This approach was also used to measure the pitch angle of the bullet prior to impact.

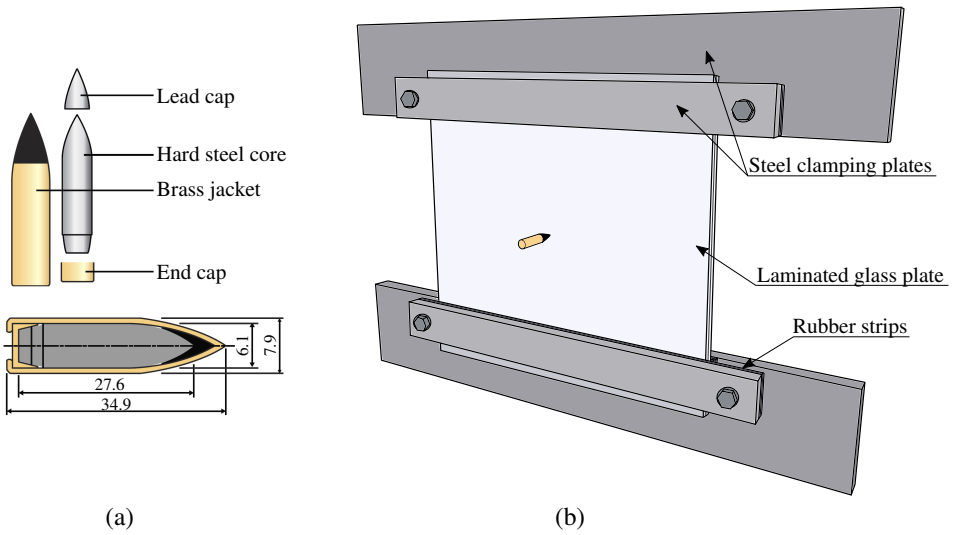

Figure 2: Illustration of the ballistic test setup: (a) 7.62 mm AP bullet (dimensions given in mm) [29], (b) clamping of the laminated glass plate.

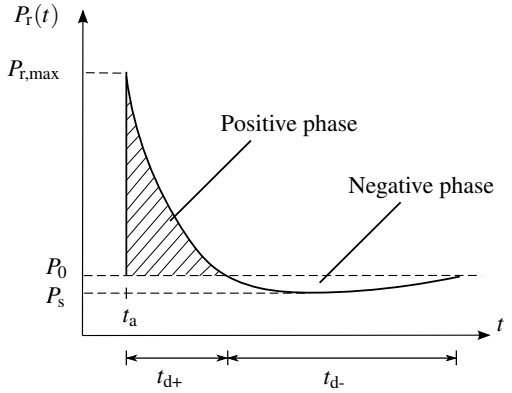

Figure 3: Idealized pressure-time history for the reflected blast wave from an explosion [7].

3.2. Blast loading

The detonation of a chemical explosive results in a rapid release of energy and the development of a blast wave. The resulting reflected overpressure on a surface (i.e., the blast loading) is dependent on parameters such as the size of the charge and the standoff distance. An idealized reflected pressure-time history for a structure subjected to a blast wave is shown in Figure 3. The maximum reflected pressure $P_{\mathrm{r,\,max}}$ occurs at the arrival time t_{a} and rises from atmospheric pressure P_0 over a time period close to zero. Subsequently, the pressure decays to atmospheric pressure P_0 over a time period $t_{\mathrm{d+}}$ and further down to the negative overpressure P_{s} over a time period $t_{\mathrm{d\text{-}}}$. The first pressure phase is referred to as the positive phase, while the last is referred to as the negative phase. The positive pressure phase is frequently described by the modified Friedlander equation [7], given by

$$P_r(t) = P_0 + P_{\mathrm{r,\,max}}\left(1 - \frac{t - t_a}{t_{d+}}\right)\exp\left(\frac{-b\,(t - t_a)}{t_{d+}}\right) \tag{1}$$

where b governs the curvature from $P_{\mathrm{r,\,max}}$. In this study, the obtained blast loadings have a negligible negative pressure phase, and the modified Friedlander equation is sufficient to describe the pressure loading. It should, however, be noted that the negative phase may have a pronounced effect on the blast response of glass plates (see, e.g., [33]). In further references to Equation 1, we will employ the reflected overpressure, i.e., $P(t) = P_r(t) - P_0$. Additionally, the time of arrival t_{a} is set to 0. The maximum reflected overpressure will be denoted P_{max}.

3.3. Blast load tests

The SIMLab Shock Tube Facility (SSTF) was used to subject the laminated glass plates to blast loading similar to that from a far-field explosion. The SSTF has earlier been proven to produce planar pressure loadings onto specimens, and is a reliable and safe alternative to explosive detonations. The following text provides some information about the SSTF, and the reader is also referred to the work by Osnes et al. [18] or Aune et al. [34] for a more thorough description.

Figure 4 shows pictures of the SSTF and includes a sketch of the different parts of the shock tube as well. It consists of a high-pressure chamber (the driver), a firing section, a low-pressure chamber (the driven), a window section, and finally, a dump tank. The test specimen is attached to the end of the driven and is positioned inside the tank. The tests are carried out in the following order: (1) one or more plastic diaphragms are placed inside the firing section to separate the driver and driven; (2) air pressure (with a magnitude of P_{d}) is built up in the driver; (3) the diaphragms are ruptured by controlled venting of the firing section; (4) pressure waves travel down the driven and eventually take the form of a characteristic blast wave; (5) the blast wave is reflected at the specimen mounted at the end of the driven, and the pressure intensity is increased. The reflected overpressure represents the loading experienced by the specimen. To estimate the loading, pressure data from two pressure sensors (with a logging frequency of 500 kHz) are used to fit the Friedlander equation (Equation 1) and extrapolated to the arrival time of the blast wave at the specimen. The arrival time is estimated by assuming a constant velocity of the blast wave between the pressure sensors and the specimen. The two pressure sensors (denoted Sensors 1 and 2) are placed 245 mm and 345 mm upstream from the plate and 150 mm above the midpoint of the tested specimen; see Figure 4a. The pressure loading is dependent on the built-up driver pressure P_{d} and the volume of the driver, both of which can be varied to achieve the desired pressure loading [34]. During testing of the laminated glass, the tank is closed, and two Phantom v1610 or v2511 high-speed cameras, synchronized to each other and to the pressure recordings, are placed outside to film through windows in the tank. The recording rate of the cameras is set to either 24 kHz (v1610) or 37 kHz (v2511) in these tests. The pressure is measured by Kistler 603B piezoelectric pressure sensors with Kistler 5064 charge amplifiers and a data acquisition system from National Instruments (NI USB-6356). More details regarding the pressure measurements in the shock tube

are given by Aune et al. [34].

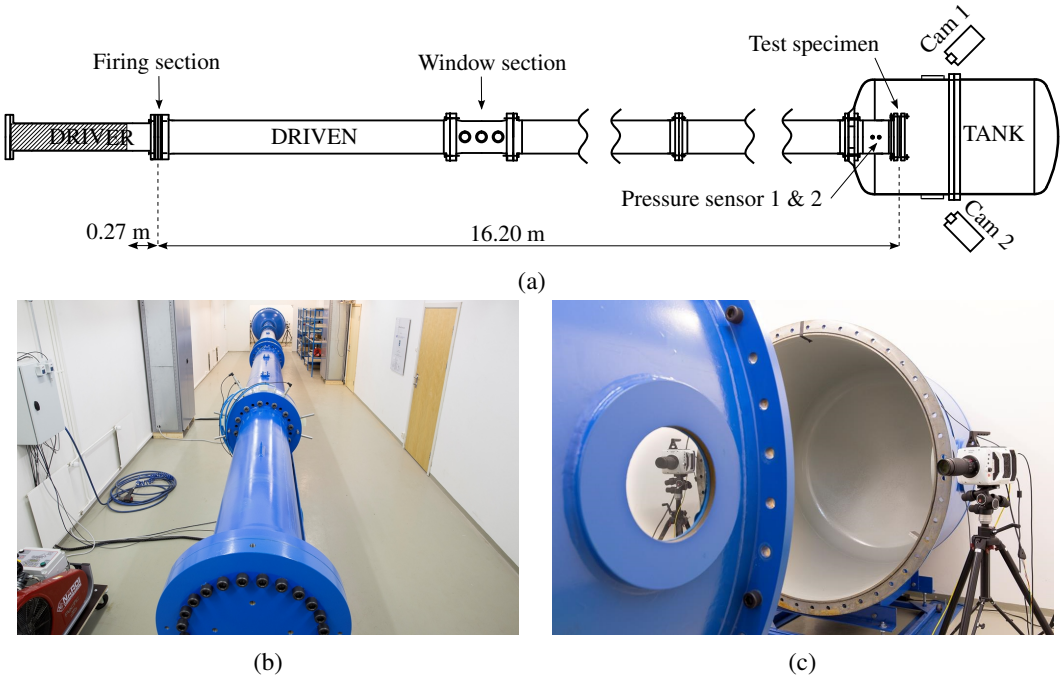

Figure 4: Test setup in the SIMLab Shock Tube Facility (SSTF) [18, 34]: (a) sketch of the shock tube seen from above, (b) the shock tube seen from the driver, and (c) high-speed cameras on each side of the tank.

The fastening system shown in Figure 5 has been developed to test glass plates in the SSTF. The specimen is clamped between two 25 mm thick steel plates, referred to as the inner and outer clamping plate. The inner clamping plate is placed closest to the driven and includes a 5.7 mm deep milled-out area to facilitate the setup. Neoprene rubber strips with a thickness of 4 mm and a width of 50 mm are glued to each clamping plate and positioned on each side of the glass. In these tests, the in-plane area of the glass specimen is 400 mm $\times$ 400 mm, while the loaded area is 300 mm $\times$ 300 mm. The outer clamping plate is fastened with 12 M24 bolts with a fixed distance of 260 mm from the centre of the glass specimen. The total radius of the clamping plates is 325 mm. On each of the bolts, we placed steel stoppers (with a diameter of 43 mm and a thickness of 11.8 mm) in order to limit the pressure on the rubber and glass while simultaneously being able to properly tighten the clamping plates together. The thickness of the steel stoppers was motivated by a clamping pressure of 14 ± 3 N/cm^2, specified in the European standard for testing of security glazing [35]. Since the thickness of the steel stoppers will control the compression of the rubber

strips, it will also control the clamping pressure. To obtain the exact clamping pressure proved, however, to be difficult due to small variations in the thickness of the glass plate, rubber strips and clamping plate. Nonetheless, the stoppers provided a fixed test setup with proper fastening without damaging the glass plates prior to testing.

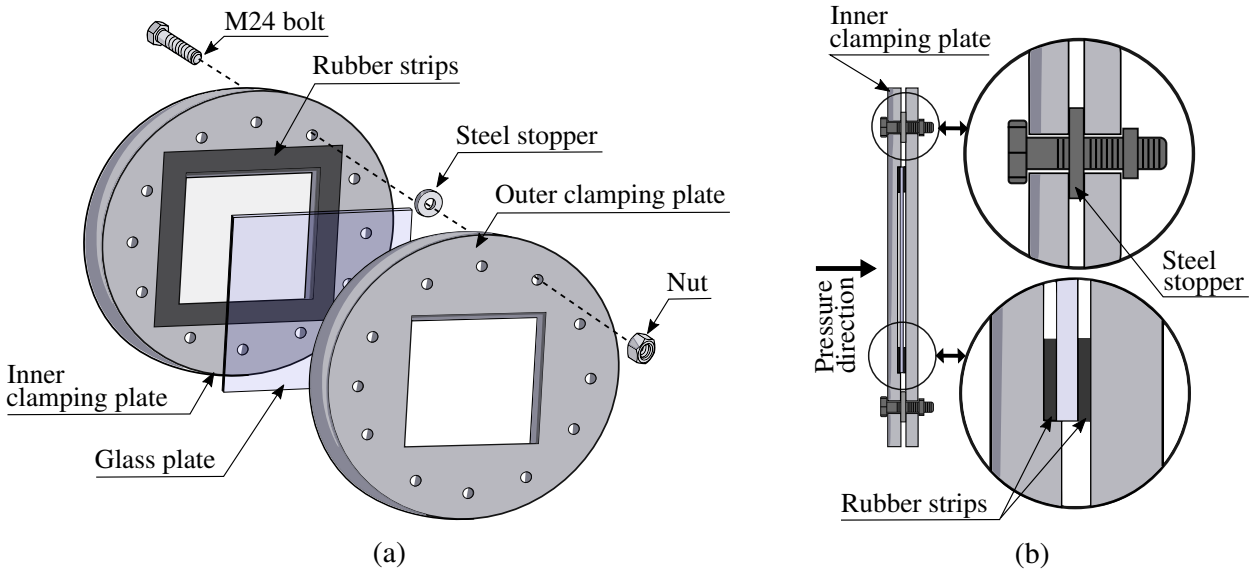

Figure 5: Illustration of the fastening system used in the blast experiments on glass in the SSTF [18]: (a) disassembled setup showing one of 12 bolts, stoppers and nuts, (b) assembled section observed from the side.

3.4. DIC measurements

A three-dimensional point-tracking procedure was employed to obtain the deformation of the laminated glass plates during blast loading. A total of 25 white circles with a central black dot (denoted optical targets) were painted on the glass, while the in-house 3D digital image correlation (DIC) software eCorr [32] was used to track their displacements. The optical targets had a diameter of 15 mm, while the distance between them was c/c 60 mm in both the transverse and longitudinal direction. This procedure was previously validated and proven valid against laser measurements [18]. Note that a point-tracking procedure is chosen instead of a more traditional 3D-DIC measurement technique, which gives the complete displacement field. This selection is done because the traditional method needs a speckle pattern that would partly obstruct the visibility of the crack initiation and propagation during blast loading of the brittle glass plates.

3.5. Test programme

In this study, a total of 11 laminated glass plates were tested in the SSTF. Five of them were initially undamaged, while two included a 5 mm diameter centrally placed hole generated by a diamond drill. The last four laminated glass plates were centrally impacted by 7.62 mm AP bullets (with and without the brass jacket) fired from a Mauser rifle. The details of the impact tests are given in Section 3.1. Note that the blast loading was applied to the same side as the bullet impact, i.e., the front side. All plates had in-plane dimensions of 400 mm $\times$ 400 mm and included two 3.8 mm thick annealed float glass plates with a 1.52 mm thick PVB interlayer. Table 1 presents an overview of the tests performed in the SSTF, with information about the desired driver pressure P_d and the imposed damage. Note that the actual driver pressure may differ slightly from the desired pressure since the diaphragms are not instantaneously removed and that the volume of the driver will increase slightly due to deformation of the diaphragms before rupture. The initial volume of the driver was the same for all the tests (i.e., a driver length of 0.27 m [34]).

Table 1: Overview of the experiments performed in the SSTF.

Test	P_d (kPa)	Imposed damage
L01a	860	Undamaged
L01b	860	Undamaged
L02	1000	Undamaged
L03	1200	Undamaged
L04	1500	Undamaged
H01	860	5 mm drilled hole
H02	1000	5 mm drilled hole
AP01	860	Bullet (7.62 mm AP) perforation
AP02	1000	Bullet (7.62 mm AP) perforation
CO01	860	Bullet (core only) perforation
CO02	1000	Bullet (core only) perforation

4. Experimental results

4.1. Ballistic impact tests

Table 2 presents the measured initial (v_i) and residual (v_r) velocities of the bullet from the four ballistic impact tests. It is seen that the reduction in bullet velocity during the perforation process is rather low, meaning that the applied laminated glass does not offer much ballistic resistance. This finding demonstrates that perforation of similar laminated glass by a fragment generated by a high-explosive detonation is very likely. Table 2 also shows that the tests with the full AP bullet (i.e., Test 1 and Test 2) had higher initial velocities than those with the CO bullet (i.e., Test 3 and Test 4) resulting from an imprecise adjustment of the ammunition. As a consequence, the initial kinetic energy of the AP bullets was more than three times that of the CO bullets. Additionally, the bullet in Test 4 impacted the laminated glass with a pitch angle of 4.5 degrees, which is normally considered too high in standard ballistic testing. However, this is of minor importance in this study, as the main purpose of the ballistic tests was to impact and perforate the laminated glass before blast loading. Consider also that a fragment will have an arbitrary shape and impact angle and that the perforation capability depends somewhat on these factors. Moreover, the appearance, i.e., the crack pattern and the penetration channel, turned out to be highly similar for the four ballistic impact tests. This similarity is shown in Figure 6, which presents pictures of the laminated glass after ballistic testing. The pictured side is the one being impacted, i.e., the front side. It was observed that the diameter of the holes induced in the PVB interlayer by the perforating bullets was smaller than the 5 mm diameter hole drilled into the laminated glass (see Section 3.1) due to the viscoelastic material behaviour of the PVB.

Figure 7 shows high-speed camera images from Test 1 (AP bullet) and Test 3 (CO bullet) at six different time points. The pixel-to-millimetre ratio in the images is approximately 32.5, while the resolution is 1024×224 pixels. The pitch angle prior to impact was negligible in these tests. It appears that the front plate of the laminated glass was crushed more extensively by the CO bullet than by the full AP bullet, presumably due to the plastic sabot not being stripped before impact. Further, the amount of fracture at the backside seems larger for the AP bullet tests than for the CO bullet tests, which was probably a result of the larger projectile diameter. In both cases,

severe local fragmentation from both sides of the laminated glass was observed. The high-speed camera images reveal that the amount of damage in the hard bullet core after the impact was negligible. Finally, it appears that the brass jacket of the full AP bullet was partly stripped during the perforation process.

Table 2: Initial (v_i) and residual (v_r) velocities in the ballistic impact tests.

Test	v_i (m/s)	v_r (m/s)	Shock tube test
1	891.7	858.3	AP01
2	892.3	859.0	AP02
3	732.7	658.7	CO01
4	671.7	571.9	CO02

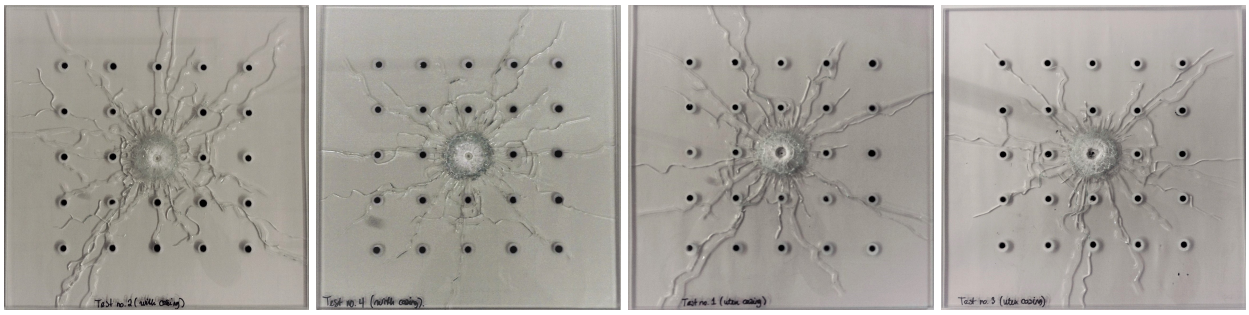

(a) Test 1 (b) Test 2 (c) Test 3 (d) Test 4

Figure 6: Laminated glass plates after the ballistic impact tests. The two first plates in (a) and (b) were impacted by AP bullets, while the two last plates in (c) and (d) were impacted by CO bullets.

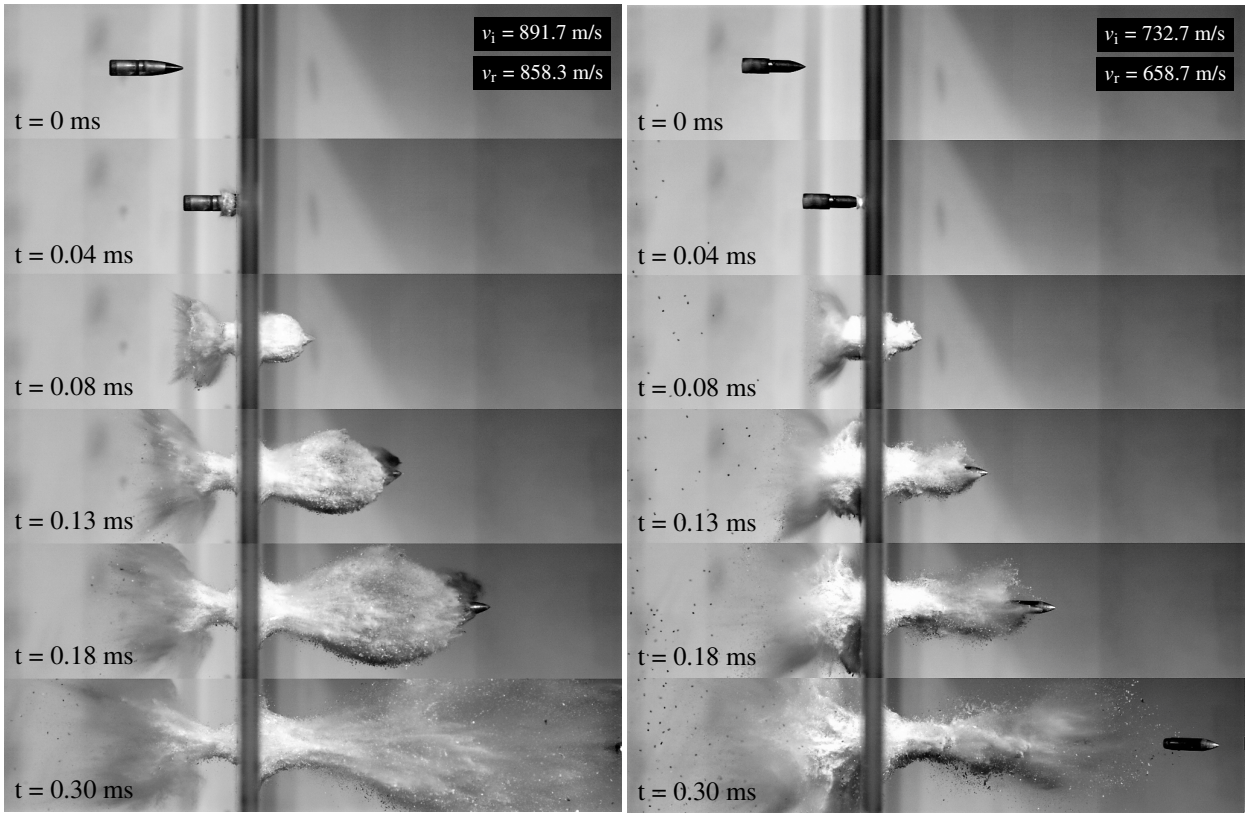

(a) (b)

Figure 7: High-speed camera images of the perforation process of the laminated glass by (a) an AP bullet (Test 1) and (b) a CO bullet (Test 3).

4.2. Blast load tests

Figure 8 presents the pressure readings in Sensor 1 from all 11 blast tests, subdivided into four plots based on the driver pressure P_d. Note that the sensor is located 245 mm from the specimen and therefore registers both the incident blast wave (at $t < 0$) and the reflected blast wave (at $t > 0$). The figure also includes curve fits of the Friedlander equation (Equation 1), which represent the reflected overpressure (i.e., the blast loading) on the laminated glass plates. It is seen that tests with the same desired driver pressure P_d resulted in an almost identical pressure reading in Sensor 1 and consequently the same parameters of the Friedlander equation, confirming the repeatability of the SSTF. In the tests with a desired driver pressure P_d of 860 kPa and 1000 kPa, the actual driver pressure was $859 \pm 2\%$ kPa and $1001 \pm 3.7\%$ kPa, respectively. The maximum reflected overpressure was $215.2 \pm 2.5\%$ kPa and $254.2 \pm 4\%$ kPa. The Friedlander parameters are presented

in Table 3. Note that the setup for Tests L01a and L01b was identical. However, no glass fracture was observed in Test L01a, whereas for Test L01b, both glass plates fractured, demonstrating the stochastic fracture behaviour of glass. The Friedlander equation for Test L04 (Figure 8d) is only partially fitted due to a rapid drop in pressure after approximately 8 ms (indicated by a cross on the Friedlander curve fit). This sudden drop in pressure is due to a complete rupture of the PVB interlayer, which in turn allows the pressure to freely pass through the laminated glass, as there is no longer a surface on which to reflect the pressure.

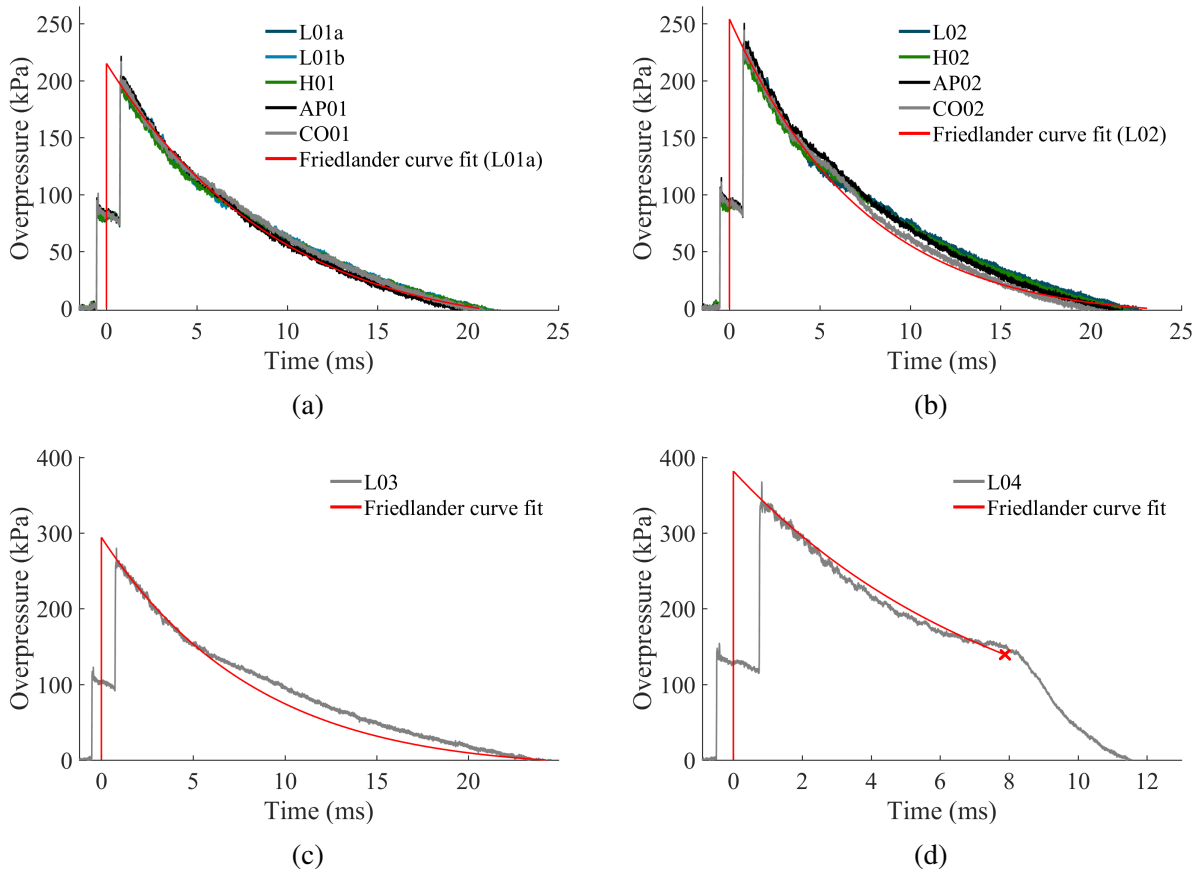

Figure 8: Pressure measurements in Sensor 1, including a representation of the reflected overpressure by a curve fit of the Friedlander equation for tests with P_d equal to (a) 860 kPa, (b) 1000 kPa, (c) 1200 kPa and (d) 1500 kPa.

Table 3: Parameters of the Friedlander equation for the blast tests in the SSTF.

Test	P_d (kPa)	P_{max} (kPa)	t_d (ms)	b (-)
L01a	860	215.2	20.62	1.42
L02	1000	254.2	20.78	1.51
L03	1200	294.5	24.02	2.04
L04	1500	382.1	×	×

We start by considering the five blast tests on the laminated glass without imposed damage (see Table 1). At the lowest overpressures, i.e., $P_{max} < 300$ kPa, the PVB interlayer was intact after testing, meaning that the pressure did not pass through the protection even if both glass plates fractured and the laminated glass was severely damaged. However, as already mentioned, at an overpressure of approximately 380 kPa, the PVB interlayer ruptured, allowing the pressure to freely pass through the protection. Thus, for this test setup, the total capacity of the initially undamaged laminated glass lies at an overpressure somewhere between 300 kPa and 380 kPa. It should be mentioned that although the fracture process of the glass plates is known to be highly stochastic [18], the rupturing of the PVB interlayer is assumed not to be. High-speed camera pictures at various points in time from the tests on the initially undamaged laminated glass are given in Figure 9, Figure 10 and Figure 11. The pixel-to-millimetre ratio in the images is approximately 1.9, while the resolution is 768×800 pixels. It is seen that before the PVB interlayer ruptures in Test L04 (see Figure 11), a large number of glass fragments are detached and launched from the protection. This phenomenon occurs on both sides of the PVB interlayer. Detachment of glass fragments is also observed in Test L03. The fragments have similar sizes, but the number of fragments is smaller than that in Test L04. Moreover, Tests L01b and L02 generated more powder-like fragments. Pictures from Test L01a, where failure did not occur in any of the glass plates, are not shown for brevity.

Next, we compare the response of the pre-damaged and the undamaged laminated glass plates exposed to blast loading. The pressure readings in Figure 8a-b suggest that there is no particular pressure decrease at Sensor 1 due to the imposed damage in the laminated glass. However, the

overall response of the plates is highly altered. This finding is illustrated in Figures 9 and 10, which include pictures at four points in time from the different tests. The pictures show that the specimens without imposed damage (L01b and L02) fractured into tiny fragments over most of the plate surface, whereas for the damaged plates, the fragments were in general much larger and more similar to those observed from ordinary annealed float glass [18]. More seriously, the pre-induced damage led to tearing of the PVB interlayer already at the lowest blast loading ($P_{\max} = 215$ kPa) and more so as the pressure was increased. Furthermore, the laminated glass pre-damaged by bullets were, as expected, more destroyed than those pre-damaged by drilled holes. In the former, the PVB ruptured over a larger area, and the glass fractured into larger pieces. This in turn led to detachment of more and larger glass fragments. It was also observed that fracture in the plates with pre-drilled holes initiated exactly at the hole. This observation indicates that the drilling generated micro-cracks since fracture initiation normally results from stress concentrations around pre-existing cracks. For the bullet-impacted plates, several cracks were clearly visible before testing (see Figure 6), and fracture in the glass initiated at several places at the same time.

In contrast to Test L04, none of the pre-damaged plates exhibited complete rupture of the PVB interlayer, and a rapid drop in pressure at Sensor 1 was not observed. This result is probably because Sensor 1 is located some distance from the centre of the laminated glass and because there was still some glass surface from which to reflect pressure in these tests. It is reasonable to believe that if the pressure sensor was located closer to the plate's centre, a pressure drop would have been visible.

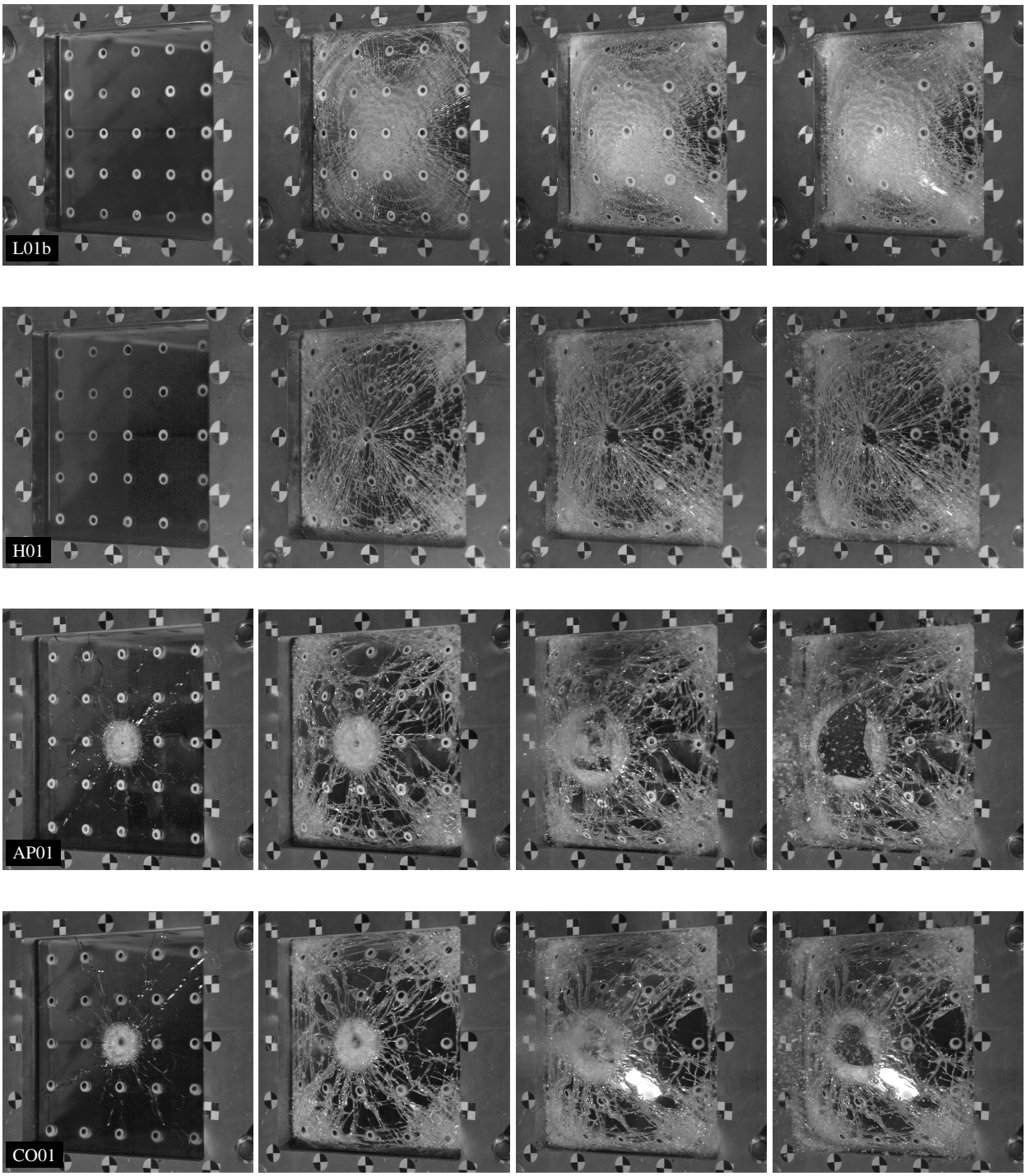

(a) 0 ms (b) 3.0 ms (c) 6.0 ms (d) 9.0 ms

Figure 9: Recorded photos of tests with P_d = 860 kPa captured at various points in time (see subcaptions) after t_a.

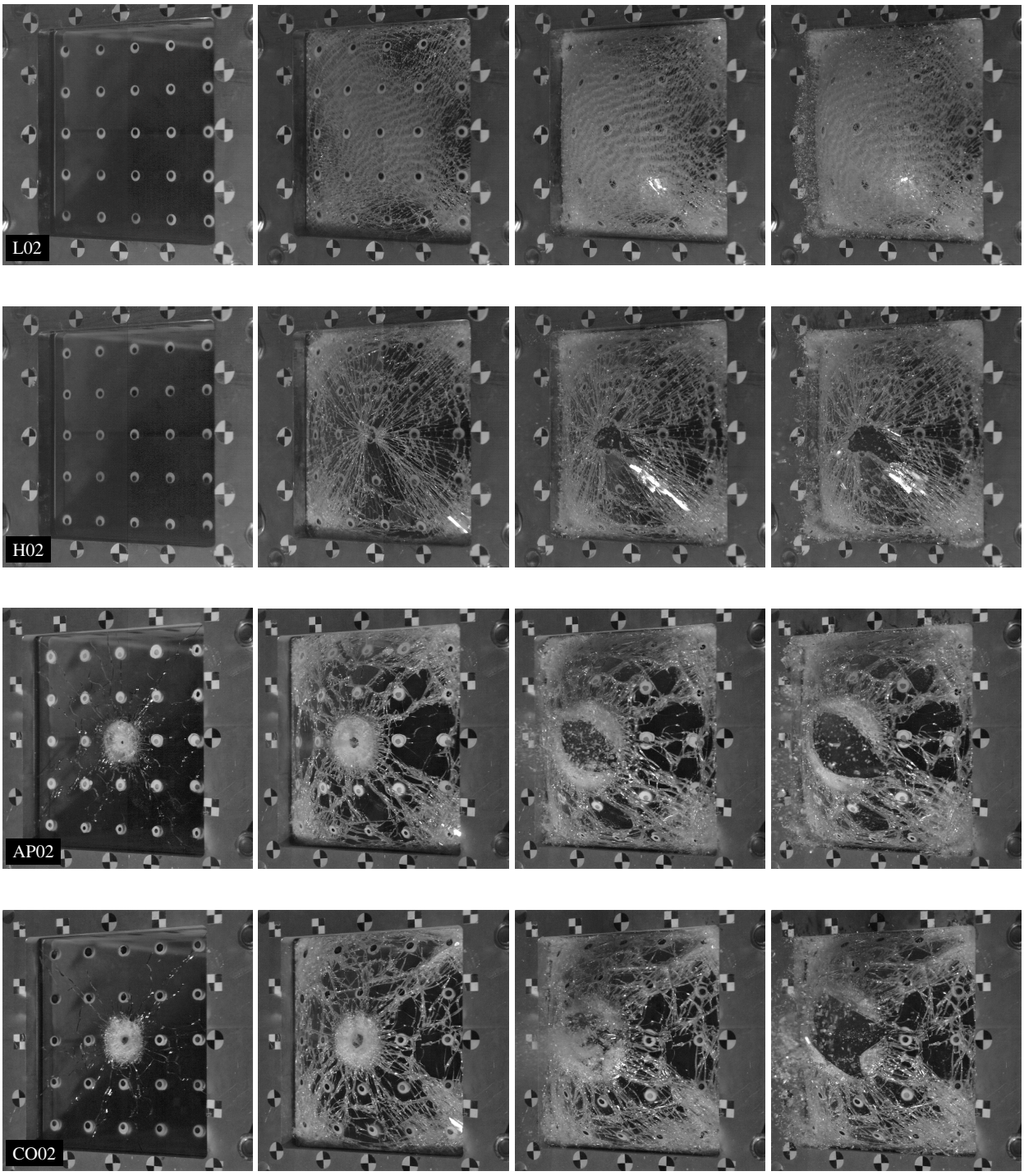

(a) 0 ms (b) 3.0 ms (c) 6.0 ms (d) 9.0 ms

Figure 10: Recorded photos of tests with P_d = 1000 kPa captured at various points in time (see subcaptions) after t_a.

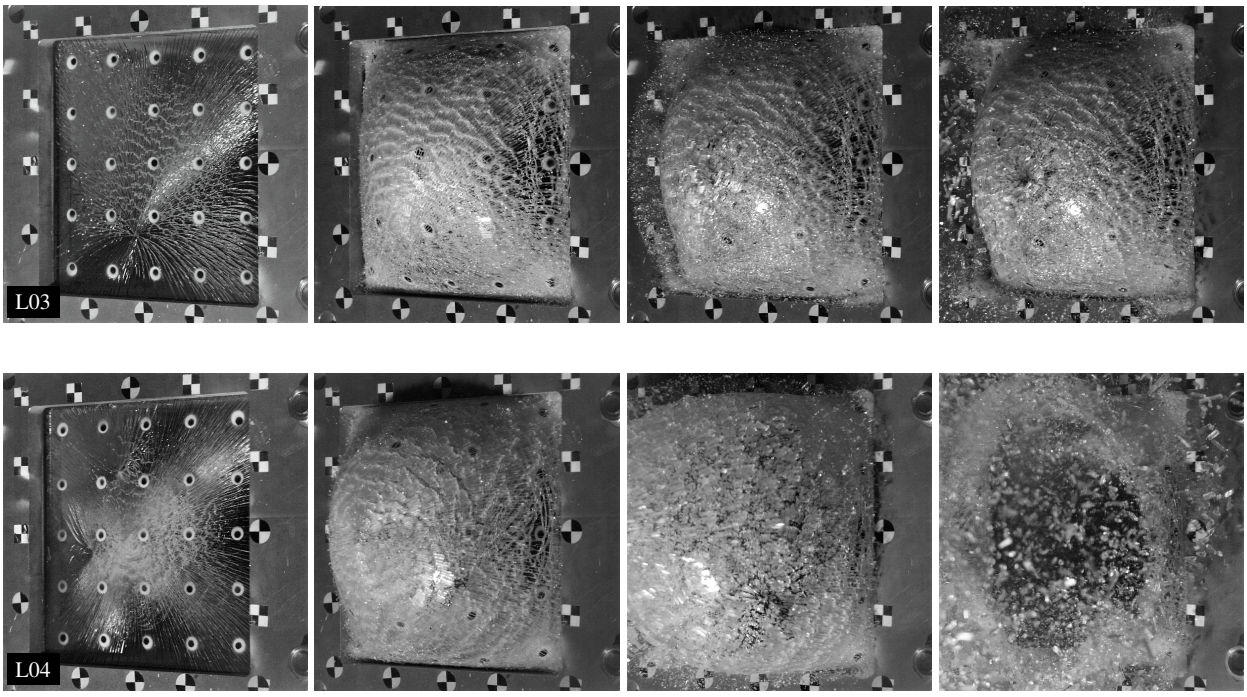

(a) 1.0 ms (b) 5.0 ms (c) 8.0 ms (d) 14.0 ms

Figure 11: Recorded photos of Tests L03 and L04 with P_d = 1500 kPa captured at various points in time (see subcaptions) after t_a.

It is clear from the pictures in Figure 9 and Figure 10 that the protective capability of the laminated glass is severely decreased if pre-damaged by fragment or bullet impact before being blast loaded since larger glass splinters are generated and detached from the PVB interlayer. Additionally, the pressure can freely pass through the protection in all cases. At these pressures, the initially undamaged laminated glass is still intact. Pictures of some representative laminated glass specimens after blast loading are shown in Figure 12. It is seen that the PVB displays viscoelastic behaviour, with nearly no permanent deformation some time after the blast tests. The specimens also appear to be highly damaged, especially the one from Test L04. It should, however, be kept in mind that since the SSTF is a closed system, the blast wave will not disappear after the first impact. Instead, it will propagate back and forth inside the shock tube until equilibrium is re-established, and the laminated glass may be impacted several times but with decreased intensity. Thus, pictures after testing such as those shown in Figure 12 can be misleading, as the damage may be exaggerated.

Finally, Figure 13 presents average out-of-plane displacements versus time for four optical targets (shown in Figure 13c) during blast loading. These results are obtained by using the point-tracking procedure described in Section 3.4. The central optical target could not be tracked due to the pre-damage. As seen, when the glass plates do not fail (i.e., Test L01a), the displacements are negligible. However, when they do fail, the displacements become significant, and the blast loading is carried by membrane stretching of the ductile interlayer. Furthermore, when the laminated glass was pre-damaged, the displacement seemed to increase with the degree of initial damage, as the displacements of the glass plates pre-damaged by bullets were higher than those for the glass plates pre-damaged by a drilled hole. The displacement of the initially undamaged laminated glass plates that failed falls between those of the plates with pre-drilled holes and the plates pre-damaged by the bullets. It must be emphasized that the latter would not necessarily hold for a rerun of the undamaged plate tests. As previously mentioned, fracture in glass is a highly stochastic process, which results in variation in the position of fracture initiation. Furthermore, the position of initiation will affect the rest of the displacement history. It is also expected that the properties of the pre-induced damage will affect the overall behaviour of the laminated glass. These properties include the size, the amount, and the location of the damage.

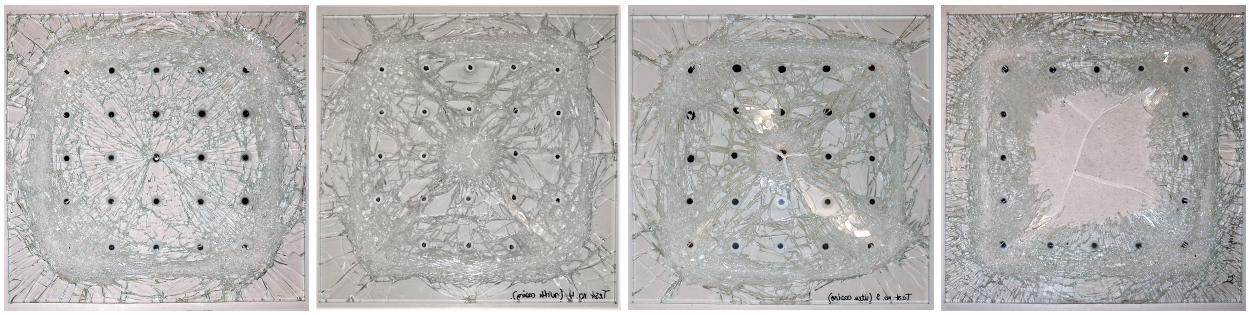

(a) (b) (c) (d)

Figure 12: Pictures of typical laminated glass specimens after blast loading for Tests (a) H02, (b) AP02, (c) CO02 and (d) L04. The pictured side is the one facing towards the cameras in the shock tube tests (backside).

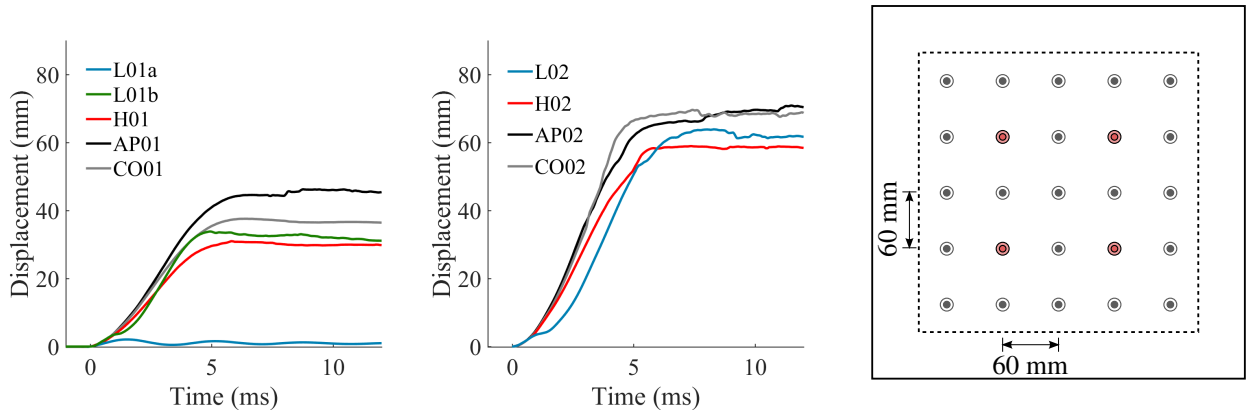

(a) (b) (c)

Figure 13: Average out-of-plane displacement of four optical targets from tests with P_d equal to (a) 860 kPa and (b) 1000 kPa, while (c) shows the position of the four optical targets (marked in red) on the glass surface used in the measurements.

5. Concluding remarks

Whenever a high explosive detonates, an intense blast wave accompanied by free-flying fragments is generated. These fragments may have velocities and masses similar to bullets fired from rifles. Since the velocity of the propagating blast wave decays rapidly, the fragments will break through the shock front and impact any target before arrival of the blast wave if the detonation is far-field. If this target is laminated glass, mainly intended for blast protection, the fragment will most likely fracture the glass plates and perforate the interlayer. Upon arrival of the subsequent blast wave, the PVB interlayer in the damaged window may rupture completely, allowing the pressure to enter the structure together with large glass fragments detached from the laminate. Thus, the protective capability of the laminated glass may be lost if pre-damaged by fragment or bullet impact before being blast loaded.

This supposition has been proven experimentally in the current study. First, we blast loaded laminated glass (consisting of two 3.8 mm thick annealed float glass plates and a 1.52 mm thick PVB interlayer) successively in a shock tube until the laminate ruptured to determine the capacity against blast loading. Then, we pre-damaged several laminated glass specimens, either by drilling a 5 mm hole in the centre of the specimens using a diamond drill or by firing two different types of

bullets at them. Lastly, the pre-damaged plates were blast loaded using the same pressures as those in the tests of the initially undamaged windows. It was found that the glass in the pre-damaged plates broke into larger fragments than the glass in the undamaged ones. This effect seemed to increase the amount and size of glass fragments detached from the PVB interlayer. Furthermore, the damage to the PVB was severely increased with the amount of pre-damage in the laminated glass. This in turn allowed the blast pressure to pass freely through the barrier. The protective capacity of the laminated glass is thus clearly reduced if it is pre-damaged by a fragment or a bullet. It is therefore highly recommended to consider fragment impact as well in the design of blast-protective windows.

Acknowledgement

The present work has been carried out with financial support from the Centre of Advanced Structural Analysis (CASA), Centre for Research-based Innovation, at the Norwegian University of Science and Technology (NTNU) and the Research Council of Norway through project no. 237885 (CASA). The authors would like to acknowledge Mr. Trond Auestad for assisting with the experimental programme, and Modum Glassindustri for providing the glass specimens.

[1] P. A. Hooper, R. A. M. Sukhram, B. R. K. Blackman, J. P. Dear, On the blast resistance of laminated glass, International Journal of Solids and Structures 49 (6) (2012) 899–918.

[2] S. M. Wiederhorn, Fracture surface energy of glass, Journal of the American Ceramic Society 52 (2) (1969) 99–105.

[3] M. Larcher, G. Solomos, F. Casadei, N. Gebbeken, Experimental and numerical investigations of laminated glass subjected to blast loading, International Journal of Impact Engineering 39 (1) (2012) 42–50.

[4] X. Zhang, H. Hao, Z. Wang, Experimental study of laminated glass window responses under impulsive and blast loading, International Journal of Impact Engineering 78 (2015) 1–19.

[5] J. Pelfrene, J. Kuntsche, S. Van Dam, W. Van Paepegem, J. Schneider, Critical assessment of the post-breakage performance of blast loaded laminated glazing: experiments and simulations, International Journal of Impact Engineering 88 (2016) 61–71.

[6] Wikipedia, `https://en.wikipedia.org/wiki/2011_Norway_attacks`, Accessed: 2018-07-07.

[7] D. Cormie, G. Mays, P. D. Smith, Blast effects on buildings, 2nd Edition, Thomas Telford Publishing, 2009.

[8] U.S. Army, TM5-855-1, Fundamentals of protective design for conventional weapons, Chapter 7: Fragmentation, Technical Manual.

[9] W. Arnold, E. Rottenkolber, Fragment mass distribution of metal cased explosive charges, International Journal of Impact Engineering 35 (12) (2008) 1393–1398.

[10] H. Y. Grisaro, D. Benamou, A. N. Dancygier, Investigation of blast and fragmentation loading characteristics–field tests, Engineering Structures 167 (2018) 363–375.

[11] Z. W. Guo, G. Y. Huang, C. M. Liu, S. S. Feng, Velocity axial distribution of fragments from non-cylindrical symmetry explosive-filled casing, International Journal of Impact Engineering 118 (2018) 1–10.

[12] U. Nyström, K. Gylltoft, Numerical studies of the combined effects of blast and fragment loading, International Journal of Impact Engineering 36 (8) (2009) 995–1005.

[13] H. Y. Grisaro, A. N. Dancygier, Characteristics of combined blast and fragments loading, International Journal of Impact Engineering 116 (2018) 51–64.

[14] J. Leppänen, Experiments and numerical analyses of blast and fragment impacts on concrete, International Journal of Impact Engineering 31 (7) (2005) 843–860.

[15] M. D. Hutchinson, The escape of blast from fragmenting munitions casings, International Journal of Impact Engineering 36 (2) (2009) 185–192.

[16] H. Y. Grisaro, A. N. Dancygier, Spatial mass distribution of fragments striking a protective structure, International Journal of Impact Engineering 112 (2018) 1–14.

[17] NS-EN 572-1: Glass in building – Basic soda-lime silicate glass products – Part 2: Float glass, Standard, CEN (2012).

[18] K. Osnes, T. Børvik, O. S. Hopperstad, Testing and modelling of annealed float glass under quasi-static and dynamic loading, Engineering Fracture Mechanics 201 (2018) 107–129.

[19] J. B. Wachtman, W. R. Cannon, M. J. Matthewson, Mechanical Properties of Ceramics, 2nd Edition, John Wiley & Sons, 2009.

[20] NS-EN 572-1: Glass in building – Basic soda-lime silicate glass products – Part 1: Definitions and general physical and mechanical properties, Standard, CEN (2012).

[21] G. Anstis, P. Chantikul, B. R. Lawn, D. Marshall, A critical evaluation of indentation techniques for measuring fracture toughness: I, Direct crack measurements, Journal of the American Ceramic Society 64 (9) (1981) 533–538.

[22] M. Peroni, G. Solomos, V. Pizzinato, M. Larcher, Experimental investigation of high strain-rate behaviour of glass, in: Applied Mechanics and Materials, Vol. 82, Trans Tech Publ, 2011, pp. 63–68.

[23] X. Zhang, Y. Zou, H. Hao, X. Li, G. Ma, K. Liu, Laboratory test on dynamic material properties of annealed float glass, International Journal of Protective Structures 3 (4) (2012) 407–430.

[24] P. Del Linz, Y. Wang, P. Hooper, H. Arora, D. Smith, L. Pascoe, D. Cormie, B. Blackman, J. Dear, Determining material response for Polyvinyl Butyral (PVB) in blast loading situations, Experimental Mechanics 56 (9) (2016) 1501–1517.

[25] X. Zhang, H. Hao, Y. Shi, J. Cui, The mechanical properties of polyvinyl butyral (PVB) at high strain rates, Construction and building materials 93 (2015) 404–415.

[26] P. A. Hooper, B. R. K. Blackman, J. P. Dear, The mechanical behaviour of poly (vinyl butyral) at different strain magnitudes and strain rates, Journal of Materials Science 47 (8) (2012) 3564–3576.

[27] J. Franz, J. Schneider, Through-cracked-tensile tests with polyvinylbutyral (PVB) and different adhesion grades, in: engineered transparency international conference at glasstec, 2014, pp. 135–142.

[28] T. Børvik, S. Dey, A. Clausen, Perforation resistance of five different high-strength steel plates subjected to small-arms projectiles, International Journal of Impact Engineering 36 (7) (2009) 948–964.

[29] J. K. Holmen, J. Johnsen, S. Jupp, O. S. Hopperstad, T. Børvik, Effects of heat treatment on the ballistic properties of AA6070 aluminium alloy, International Journal of Impact Engineering 57 (2013) 119–133.

[30] M. Forrestal, T. Børvik, T. Warren, Perforation of 7075-T651 aluminum armor plates with 7.62 mm APM2 bullets, Experimental Mechanics 50 (8) (2010) 1245–1251.

[31] T. Børvik, M. Forrestal, T. Warren, Perforation of 5083-H116 aluminum armor plates with ogive-nose rods and 7.62 mm APM2 bullets, Experimental Mechanics 50 (7) (2010) 969–978.

[32] E. Fagerholt, Field measurements in mechanical testing using close-range photogrammetry and digital image analysis, Ph.D. thesis, Norwegian University of Science and Technology (NTNU), Trondheim (2012).

[33] T. Krauthammer, A. Altenberg, Negative phase blast effects on glass panels, International Journal of Impact Engineering 24 (1) (2000) 1–17.

[34] V. Aune, E. Fagerholt, M. Langseth, T. Børvik, A shock tube facility to generate blast loading on structures, International Journal of Protective Structures 7 (3) (2016) 340–366.

[35] NS-EN 13541: Glass in building – Security glazing- Testing and classification of resistance against explosion pressure, Standard, CEN (2012).